Journal of Orthopaedic Surgery and Research

RESEARCH

Open Access

GPx3 marks adipocyte lineage commitment in bone marrow stromal cells

Zhongxiang Wang[1,2†], Yangyang Hu[1†], Mao Li[3], Xiaojun Chen[2], Chengyu Zhou[1], Zhiyang Xu[4], Kai Chen[2*] and Lichuang Wu[1*]

Abstract

Background Bone marrow adipose tissue (BMAT) plays an essential role in skeletal health and systemic metabolism, particularly under conditions of ageing and osteoporosis. Despite increasing recognition of BMAT as an active endocrine organ, the molecular mechanisms underlying its formation and expansion remain incompletely understood.

Methods We conducted a transcriptomic re-analysis of publicly available datasets focused on the adipogenic differentiation of bone marrow stromal cells (BMSCs). Differential gene expression and pathway enrichment analyses were performed to identify key molecular changes. Validation was conducted at both the transcript and protein levels. Furthermore, re-analysis of single-cell RNA sequencing (scRNA-seq) data was employed to determine the cell type–specific expression of candidate genes within the bone marrow. Functional assays using RNA interference were carried out to investigate the role of glutathione peroxidase 3 (GPx3) in adipogenesis.

Results Our analysis revealed a consistent activation of oxidative stress-related pathways during adipogenic differentiation. Among the upregulated antioxidant enzymes, GPx3 was selectively increased during adipogenic—but not osteogenic—differentiation. This pattern was validated at both mRNA and protein levels in vitro. scRNA-seq analysis showed that GPx3 expression is predominantly localized in BMSCs and adipocytes, with reduced expression observed in aged mice, corresponding to elevated levels of adipocyte-related genes. In vitro functional experiments demonstrated that GPx3 knockdown significantly promoted adipogenic differentiation of BMSCs.

Conclusion These findings indicate that GPx3 is closely associated with adipocyte lineage commitment within the bone marrow microenvironment and may serve as a key modulator of BMSC fate. This study underscores the potential role of antioxidant enzymes such as GPx3 in the regulation of age-related bone-fat imbalance and highlights their relevance in metabolic bone disorders.

Keywords GPx3, ROS, Bone marrow adipose tissue, Bone marrow stromal cells

†Zhongxiang Wang and Yangyang Hu contributed equally to this work.

*Correspondence:
Kai Chen
kai.chen@uwa.edu.au
Lichuang Wu
lichuang.wu@wmu.edu.cn
[1] Department of Orthopedics, The First Affiliated Hospital of Wenzhou Medical University, Zhejiang, China
[2] School of Biomedical Sciences, The University of Western Australia, Perth, Australia
[3] Department of Obstetrics, The First Affiliated Hospital of Wenzhou Medical University, Zhejiang, China
[4] The First Clinical School, The First Affiliated Hospital of Wenzhou Medical University, Zhejiang, China

Background

Bone marrow adipose tissue (BMAT) is a metabolically active fat depot that accounts for up to 70% of adult bone marrow (BM) and can constitute as much as 30% of total body fat [1]. Unlike conventional extramedullary fat depots—such as white, brown, and beige adipose tissue—BMAT is distinct in its origin, metabolic features, and physiological roles [2, 3]. Although historically regarded as a passive "filler" within the bone marrow compartment, BMAT is highly regulated by nutrient status and increasingly recognised as a dynamic endocrine and paracrine organ with significant implications for skeletal health [4, 5]. For example, BMAT is a unique adipose subtype that exhibits significantly higher basal nutrient uptake—particularly glucose—compared to axial bone, skeletal muscle, or subcutaneous white adipose tissue [3]. BMAT expansion could lead to decreased bone mass, particularly in ageing or postmenopausal individuals with osteoporosis [6]. Mechanistically, bone marrow adipocytes (BMAds) inhibit bone formation and promote bone resorption through direct cellular interactions or by secreting soluble factors. For example, bone marrow adipogenic lineage precursors (MALPs) secrete receptor activator of nuclear factor-κB ligand (RANKL) [7] and macrophage colony-stimulating factor (MCSF) [8], both of which are critical for osteoclastogenesis and bone loss. Strikingly, genetic ablation of BMAT in mice has been shown to induce a 1,000% increase in bone mass [9], highlighting the therapeutic potential of targeting BMAT in metabolic bone diseases.

Despite the predominance of BMAT in mammalian bone marrow, our understanding of its formation remains limited compared to that of peripheral adipose tissues. BMAds originate from bone marrow stromal cells (BMSCs), which also give rise to osteoblasts [10, 11]. A widely accepted notion is that metabolic or age-related shifts in the bone marrow microenvironment leads to a "preferential" shift in lineage commitment of BMSCs towards adipogenesis rather than osteogenesis, thereby contributing to BMAT expansion and skeletal fragility [12]. Thus, strategies that inhibit adipogenic commitment without disrupting osteogenesis are highly desirable for maintaining bone integrity. The mechanisms underlying the adipogenic differentiation of BMSCs are not yet fully understood. Emerging evidence suggests that redox imbalance plays a key role in this lineage decision. Reactive oxygen species (ROS) are byproducts of cellular metabolism and are elevated during adipogenic differentiation [13]. For example, ROS produced by NADPH oxidase 4 (NOX4) could drive BMSC adipogenesis [14]. These findings implicate oxidative stress as a crucial regulator of BMSC fate, linking metabolic activity, redox signaling, and adipocyte development.

To further investigate this, we revisited a publicly available transcriptomic dataset [15] and validated the consistent activation of oxidative stress-related pathways during BMSC adipogenesis. We hypothesized that selectively targeting redox-sensitive regulators may provide a metabolic checkpoint to inhibit adipogenesis while preserving osteogenesis. Our comparative gene expression analysis revealed that glutathione peroxidase 3 (GPx3)—a key member of the glutathione peroxidase (GPx) family—was specifically upregulated during adipogenic but not osteogenic differentiation. GPx3 is a secreted selenoprotein that catalyses the reduction of hydrogen peroxide and lipid hydroperoxides, thereby maintaining extracellular redox homeostasis and influencing metabolism-sensitive signaling cascades [16]. In functional assays, GPx3 knockdown significantly enhanced adipogenic differentiation of BMSCs, supporting its role as a redox-sensitive brake on adipogenesis. Taken together, we proposed that GPx3 could serve as a key modulator of BMSC fate, representing a novel therapeutic target for suppressing BMAT accumulation and preserving bone mass.

Materials and methods

Materials and reagents

IBMX (Cat.No. I5879), insulin (Cat.No. I3536), dexamethasone (Cat.No. D4902) and Oil Red O staining solution (Cat.No. O1516) were purchased from Sigma-Aldrich. DMEM culture media were obtained from Gibco (Cat.No. 11995065). Protein markers (Cat No. 1610394) were purchased from Bio-Rad. Primary antibodies against PPARγ (Cat.No. C26H12), C/EBPα (Cat. No. D56F10), and β-actin (Cat.No. 13E5) were purchased from Cell Signaling Technology, while antibodies against GPx3 (Cat.No. AF4199) was obtained from R&D Systems. The PCR primers for *Pparg*, *Cebpa*, *Adipoq*, and *Gpx3* used in this study were purchased from Integrated DNA Technologies.

Bioinformatics and statistical analysis

The raw RNA-seq dataset (GSE113253) was retrieved from the Gene Expression Omnibus (GEO) database [15]. Normalized expression data frame was generated by Deseq2 R package in R [17]. Genes with an adjusted p-value < 0.05 and $\log_2$ fold change > 1 were considered significantly differentially expressed. Gene Ontology (GO) and Kyoto Encyclopedia of Genes and Genomes (KEGG) pathway enrichment analysis was performed using the clusterProfiler package, multiple enrichment bubble plots were generated by using ggplot2 and patchwork R packages. Normalized expression data was further clustered and visualized into heatmap plot using ClusterGVis package. Heatmaps were generated using the pheatmap package in R, displaying dynamic

expression changes across time points (0 h, 4 h, 1d, 3d, 7d, 14d). Key genes involved in adipogenesis and redox regulation—such as *GPX3*, *GPX1*, *GPX4*, *FABP4*, *CEBPA*, and *PPARG* —were highlighted. Volcano plots were generated using the ggplot2 package in R to visualize upregulated and downregulated genes. Gene Set Enrichment Analysis (GSEA) was performed using enrichplot package in R and the KEGG pathway database. Key pathways were identified as significantly upregulated during adipogenic differentiation.

Single-cell RNA sequencing (scRNA-seq) analysis was performed using the publicly available dataset (GSE145477) [18]. The raw sequencing data were preprocessed and analyzed using Seurat in R. Briefly, the data underwent quality control and filtering as previously described [19], including the removal of cells with fewer than 200 genes detected and those with more than 25% mitochondrial gene content, to exclude low-quality or dying cells (Figure S1). The gene expression data were normalized using the LogNormalize method, and principal component analysis (PCA) was performed for dimensionality reduction. Cell clustering was conducted using Uniform Manifold Approximation and Projection (UMAP) with a resolution of 0.2.

To analyze datasets from different age groups, we applied Seurat V3 to perform integrated analyses for identifying common cell types. Following the quality control and filtering procedures described above, the 3-month-old and 16-month-old datasets were combined and processed as previously described [18]. Anchors from these two datasets were defined using the FindIntegrationAnchors function, followed by integration of the datasets using IntegrateData. The integrated data was further analyzed and divided into subclusters from bone marrow cells using known marker genes (Figure S2).

Isolation and culture of mBMSCs

All the animal experiments were approved by the Animal Ethical Committee of The University of Western Australia (approval number 2022/ET000933). Mouse BMSCs (mBMSCs) were isolated from the femurs and tibias of neonatal mice (4–7 days old). Briefly, after dissecting the bilateral hind limbs, the soft tissue and cartilage at both ends of the bones were removed. The bones were then minced with scissors and flushed with culture medium. The collected cell-containing suspension was used for cell culture. After 48 h of culture, a half-medium change was performed, followed by an additional 48 h of culture. Then the adherent cell density reached approximately 70%, and the first passage was performed. When the first-generation cells reached 80–100% confluency, they were either used for experiments directly, further passaged, or cryopreserved.

Adipogenic differentiation of mBMSCs

For adipogenic differentiation, mBMSCs were seeded in 96-well or 6-well plates. Once the cells reached 100% confluence, the medium was replaced with adipogenic differentiation medium (IBMX 500 μM, insulin 10 ug/ml and dexamethasone 100 nM). The medium was changed every three days, and after 7–10 days, Oil Red O staining was used to visualize lipid droplets.

Western blot analysis

Total protein was extracted from cells using RIPA lysis buffer supplemented with protease and phosphatase inhibitors. Protein concentration was measured using a BCA protein assay kit. Equal amounts of protein were separated by SDS-PAGE and transferred onto PVDF membranes. After blocking with 5% skim milk in TBST for 1 h at room temperature, membranes were incubated overnight at 4 °C with primary antibodies targeting the proteins of interest. After three washes with TBST, membranes were incubated with HRP-conjugated secondary antibodies for 1 h at room temperature. Protein bands were visualized using an enhanced chemiluminescence (ECL) detection kit (PerkinElmer), and band intensity was quantified using ImageJ software. β-Actin was used as the internal control.

Quantitative real-time PCR (qRT-PCR)

Total RNA was extracted using TRIzol reagent according to the manufacturer's protocol. RNA concentration and purity were determined using a NanoDrop spectrophotometer. Reverse transcription was performed with a cDNA synthesis kit to generate complementary DNA (cDNA). qRT-PCR was conducted using a SYBR Green-based PCR MasterMix (Thermo Fisher Scientific) on a real-time PCR system. The cycling parameters for PCR were set as follows: 95 °C for 10 min, followed by 50 cycles of 95 °C for 15 s, 60 °C for 60 s. The specific primers used are as following: *Pparg* (forward: 5'- TCG CTGATGCACTGCCTATG -3'; reverse: 5'- GAGAGG TCCACAGAGCTGATT -3'), *Cebpa* (forward: 5'- TGG ACAAGAACAGCAACGAG -3'; reverse: 5'- CGGTCA TTGTCACTGGTCAAC -3'), *Adipoq* (forward: 5'- GTT CCCAATGTACCCATTCGC -3'; reverse: 5'- TGTTGC AGTAGAACTTGCCAG -3'), *Gpx3* (forward: 5'- CCT TTTAAGCAGTATGCAGGCA -3'; reverse: 5'- CAA GCCAAATGGCCCAAGTT -3'). The relative expression levels of target genes were analyzed using the 2^(-ΔΔCt) method, with *Actb* as the internal reference gene. Each experiment was performed in triplicate to ensure reproducibility.

GSH and GSSG detection

The GSH/GSSG ratio was detected by GSH/GSSG Ratio Detection Assay Kit (Abcam, ab205811) according to the manufacturer's instructions. In brief, cells after 5 days of adipogenic induction were lysed using a cell lysis buffer, followed by the addition of detection reagents according to the manufacturer's instructions. Fluorescence signals were then measured using a fluorescence microplate reader at Ex/Em = 490/520 nm.

Statistical analysis

Statistical analyses were conducted on data obtained from a minimum of three independent experiments. Quantitative results are expressed as mean ± standard deviation (SD). Two-tailed t-tests were conducted to assess the significance between two groups, while one-way ANOVA with Fisher's LSD post-test was used for analyses involving multiple groups, with statistical significance defined as a p-value < 0.05, both analyzed using GraphPad Prism software (version 10).

Results

Bioinformatics analysis reveals significant upregulation of oxidative stress-related pathways during adipogenic differentiation of hBMSCs

To investigate gene expression patterns and significant signaling pathways during the adipogenic differentiation of human BMSCs (hBMSCs), we reanalyzed RNA-seq data from GEO database [15]. KEGG and GO-BP analysis revealed significant differences in intracellular oxidative stress and fatty acid metabolism processes during adipogenic differentiation (Fig. 1A).

Based on these findings, we further conducted Gene Set Enrichment Analysis (GSEA) on oxidative stress-related and lipid metabolism pathways. The results demonstrated significant activation of oxidative stress-related oxidative phosphorylation, AMPK, peroxisomal and ferroptosis pathways with the activation of fatty acid metabolism (Fig. 1B-G). Collectively, our findings indicated that the oxidative stress is actively involved in the regulation of adipogenic differentiation in hBMSCs.

Significant upregulation of GPX3 during adipogenic differentiation of hBMSCs

Previous studies have demonstrated that GPx family genes can regulate the oxidative stress activity and maintaining redox homeostasis. Based on our above findings of oxidative stress activation and lipid peroxidation during the adipogenic differentiation of BMSCs, we further analyzed the expression patterns of GPx family genes and found *GPX1-4* are highly relevant with adipogenesis (Fig. 2A). Among them, only *GPX3* exhibited a significant increase in gene expression during adipogenic differentiation, suggesting a potentially specific role in this process (Fig. 2B).

To further investigate the specificity of *GPX3*, we analyzed its expression dynamics during both adipogenic and osteogenic differentiation. The results showed no significant changes in *GPX3* expression during osteogenic differentiation, indicating that its upregulation is specific to adipogenic commitment and correlates with the progression of this process (Fig. 2C). These findings suggest that *GPX3* may play a crucial role in suppressing oxidative stress levels during the adipogenic differentiation.

In vitro validation of GPx3 upregulation during adipogenic differentiation of mBMSCs

To experimentally validate the expression of GPx3 in the adipogenic differentiation of BMSCs, we first induced adipogenic differentiation of mBMSCs in vitro. Oil Red O staining at various time points confirmed the appearance of lipid droplets by day 3, which rapidly increased in size by day 7. By day 10, the accumulation of lipid droplets reached a plateau (Fig. 3A and B).

Western blot analysis showed that the adipogenic transcriptional factor PPARγ exhibited a significant increase from day 3 of differentiation, whereas C/EBPα displayed an evident upregulation as early as day 1. Notably, GPx3 was markedly upregulated on day 1 and remained at a high expression level throughout differentiation (Fig. 3C-F). To determine whether the increase in GPx3 was due to elevated gene expression or reduced degradation, we assessed its mRNA levels. Quantitative analysis revealed a significant upregulation of the adipogenic markers *Pparg*, *Cebpa* and *Adipoq* during differentiation, alongside a pronounced increase in *Gpx3* mRNA expression (Fig. 3G-J). These findings indicate that GPx3 is significantly upregulated during the adipogenic differentiation of mBMSCs, primarily due to increased transcriptional activity.

scRNA-seq data indicate a correlation between Gpx3 expression and adipogenic differentiation

Building on the in vitro evidence demonstrating the specific upregulation of *GPX3* during adipogenic differentiation, we further investigated its correlation with adipogenic processes and its association with adipocytes in bone marrow using in vivo single cell RNAseq dataset [18]. We revealed that *Gpx3* is predominantly expressed in BMSCs and adipocytes (Fig. 4A-C), whereas its expression is relatively low in osteoblasts and chondrocytes (Fig. 4D-E). This distribution pattern underscores that *Gpx3* may play a specific regulatory role in the adipogenic differentiation of BMSCs.

To investigate the differentiation trajectory of BMSCs into adipocytes, we performed pseudotime analysis

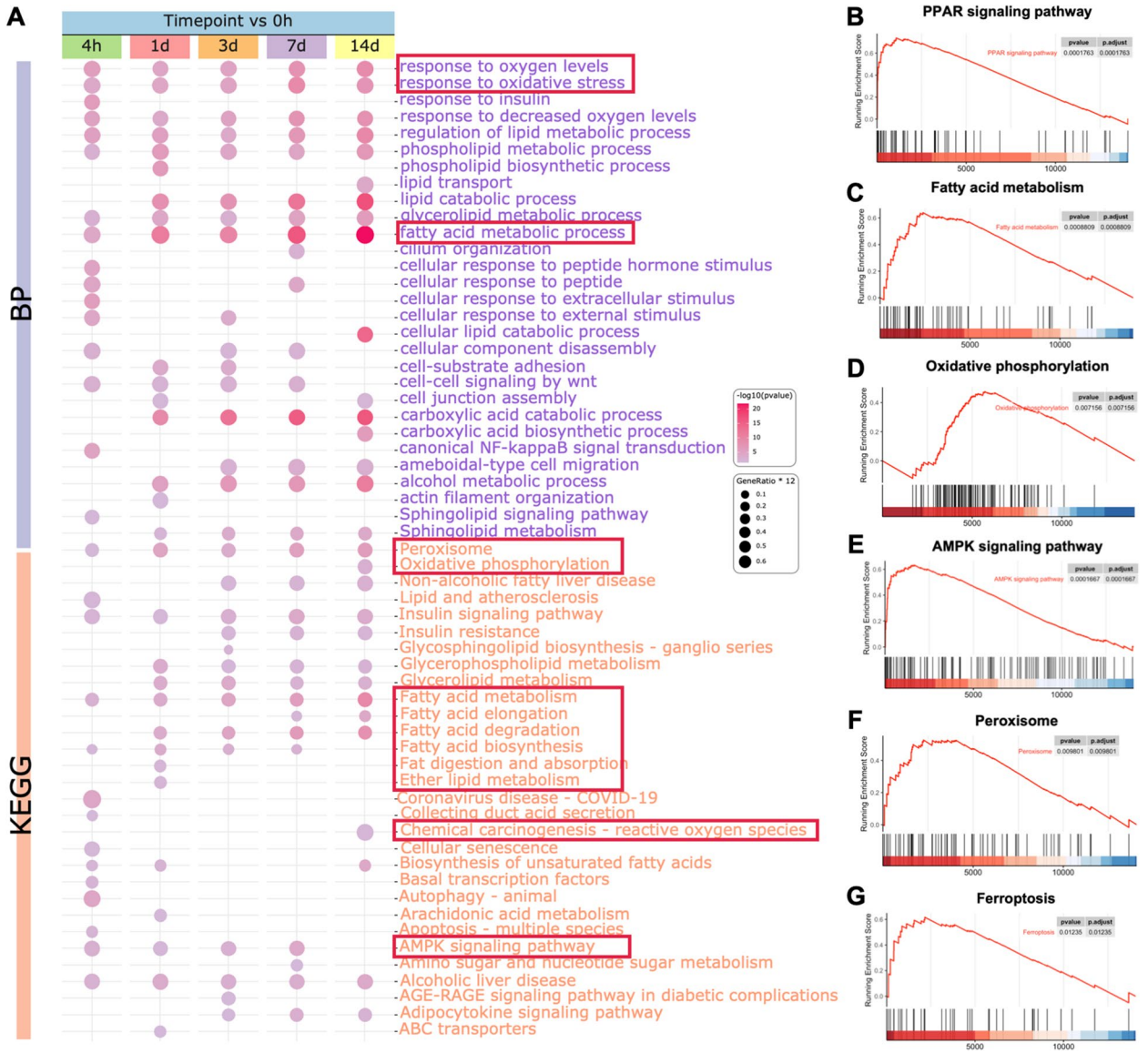

Fig. 1 Bioinformatics analysis (GSE113253) revealed that oxidative stress-related pathways were activated during adipogenic differentiation of hBMSCs. **A** GO-Biological Process and KEGG analysis results; (**B**-**G**) GESA enrichment analysis results

using Monocle3. The UMAP visualization of cell clusters (Fig. 4F) revealed distinct populations, including monocytes, neutrophils, BMSCs, osteoblasts, macrophages, B cells, platelets, chondrocytes, eosinophils, adipocytes, erythrocytes, and endothelial cells (ECs).

We analyzed the expression patterns of key genes involved in adipogenesis along these trajectories (Fig. 4G). Both *Adipoq* and *Pparg* exhibited an increasing trend in expression as BMSCs differentiated into adipocytes. Interestingly, *Gpx3* exhibited a distinctive pattern: its expression first decreased, followed by an increase as BMSCs transitioned into adipocytes. This suggests that *Gpx3* may play a key role in adipogenic differentiation. Given that adipogenic differentiation is typically accompanied by the elevated expression of adipocyte-related markers, we further analyzed the TIME2.0 database (http://timer.comp-genomics.org) to validate the association between GPX3 and adipogenesis. The analysis revealed a strong positive correlation between *GPX3* expression and the levels of adipocyte-related markers *ADIPOQ, PPARG, LPL* and *FABP4* in tumor cells, providing additional evidence that GPx3 may be critically involved in the regulation of adipogenic differentiation (Fig. 4H).

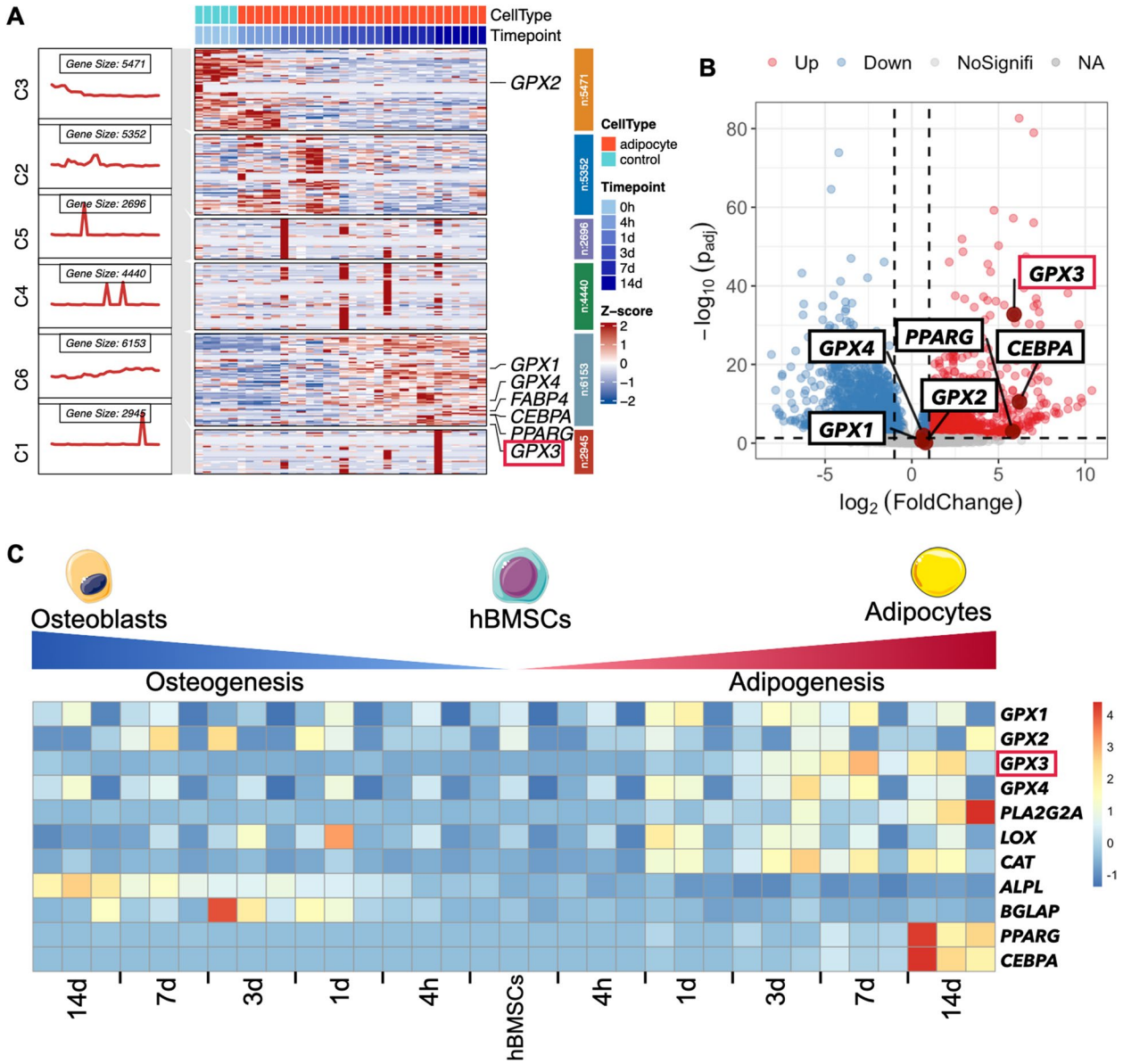

Fig. 2 Bioinformatics analysis showed that *GPX3* expression was significantly increased during adipogenic differentiation of hBMSCs. **A** Heatmap of adipogenic marker genes and GPx family genes. **B** Volcano plot of adipogenic marker genes and GPx family genes. **C** The gene expression pattern of GPx family and oxidative stress-related enzymes during osteogenic and adipogenic differentiation of hBMSCs. Oxidative stress-related enzymes genes: *PLA2G2A*, *LOX*, *CAT*; Adipogenic marker genes: *PPARG*, *CEBPA*, *FABP4*; osteogenic marker genes: *ALPL*, *BGLAP*

Gpx3 expression is markedly downregulated in BMSCs and BMAds from aged mice

It is well established that with increasing age, BMAT progressively accumulates in mice, and BMSCs exhibit a greater propensity for adipogenic differentiation. To investigate whether the enhanced adipogenic differentiation tendency of BMSCs in aged mice is associated with *GPx3*, we analyzed scRNA-seq data from the bone marrow of mice at different ages. The results indicate that the proportion of adipocytes in the bone marrow of aged mice is significantly higher than that in young mice (56.88% vs. 9.95%), while the proportion of BMSCs is relatively lower (6.67% vs. 14.40%) (Fig. 5A). Additionally, the expression levels of adipocyte marker genes *Adipoq* and *Lpl* in bone marrow cells of aged mice are significantly higher than those in young mice (Fig. 5B). UMAP dimensionality reduction analysis revealed that *Gpx3* expression is markedly reduced in *Adipoq*-positive cells (adipocytes) and *Aspn*-positive cells (BMSCs) of aged mice compared to young mice (Fig. 5C-E). Finally, violin

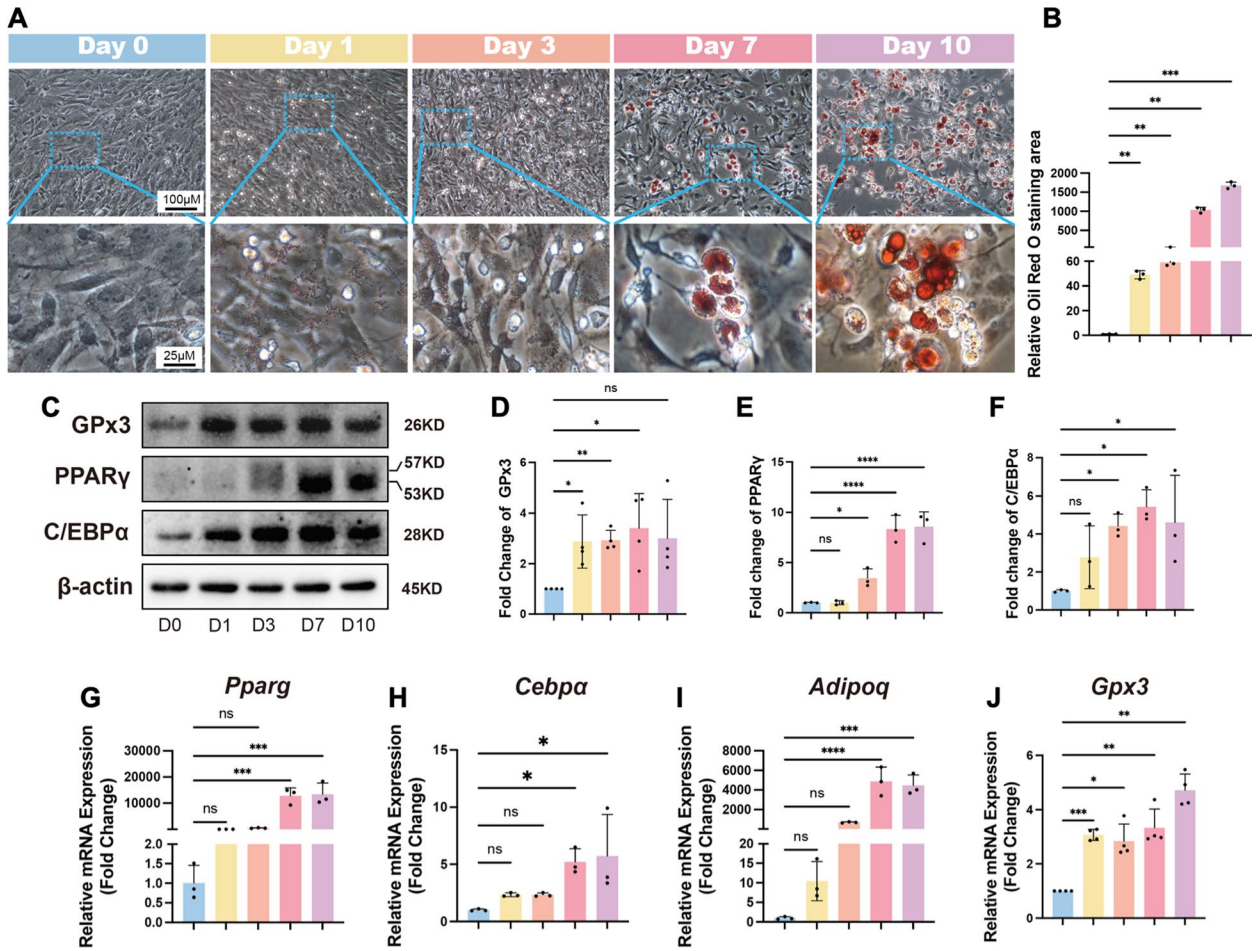

Fig. 3 GPx3 expression during adipogenic differentiation of mBMSC in vitro. **A** Representative images of Oil Red O staining at different differentiation time points and (**B**) corresponding quantification. **C** Representative Western blot images showing the protein expressions of GPx3, along with adipogenic markers PPARγ and C/EBPα, at various differentiation stages. **D**-**F** Quantifications of band intensities in (**C**). **G**-**J** Relative mRNA expression levels of *Gpx3* and adipogenic-specific genes *Pparg, Cebpa*, and *Adipoq* normalized to *Actb* during adipogenic differentiation. Data are presented as mean ± SD. **P* < 0.05, ****P* < 0.001, *****P* < 0.0001 compared to the control group; ns indicates *P* > 0.05

plot analysis further confirmed that *Gpx3* expression is significantly reduced in both BMSCs and BMAds during ageing (Fig. 5F). These findings support the notion that ageing is associated with increased BMAT formation, and that both BMSCs and adipocytes in aged bone marrow exhibit diminished *Gpx3* expression. This suggests that GPx3 may be required to maintain proper BMSC lineage commitment, potentially by restraining adipogenic differentiation under physiological conditions.

Knockdown of GPx3 significantly promotes adipogenic differentiation and enhances oxidative stress in mBMSCs

To functionally validate the role of GPx3 in adipogenic differentiation of mBMSCs, we knocked down GPx3 using siRNA, followed by adipogenic induction for 3 and 5 days. qRT-PCR analysis confirmed successful knockdown of *Gpx3* (Fig. 6A). Furthermore, the expression of adipogenic markers *Pparg*, *Cebpa*, and *Adipoq* were significantly elevated on days 3 and 5 after differentiation (Fig. 6B-D). Oil Red O staining further validated that GPX3 knockdown markedly enhanced adipogenic differentiation of mBMSCs (Fig. 6E and F). This is consistent with Western blot analysis which revealed that the GPx3 deficiency led to a significantly increased expression of key adipogenic proteins PPARγ and C/EBPα (Fig. 6G-I). To investigate whether GPx3 knockdown affects oxidative stress levels in adipocytes, we measured the GSH/GSSG ratio on day 5 of adipogenic differentiation. The results showed that GPx3 knockdown significantly reduced the GSH/GSSG ratio, indicating an increase in oxidative stress (Fig. 6J). Together, these results suggest that GPx3 plays a crucial role in regulating adipogenesis in BMSCs by modulating intracellular oxidative stress levels.

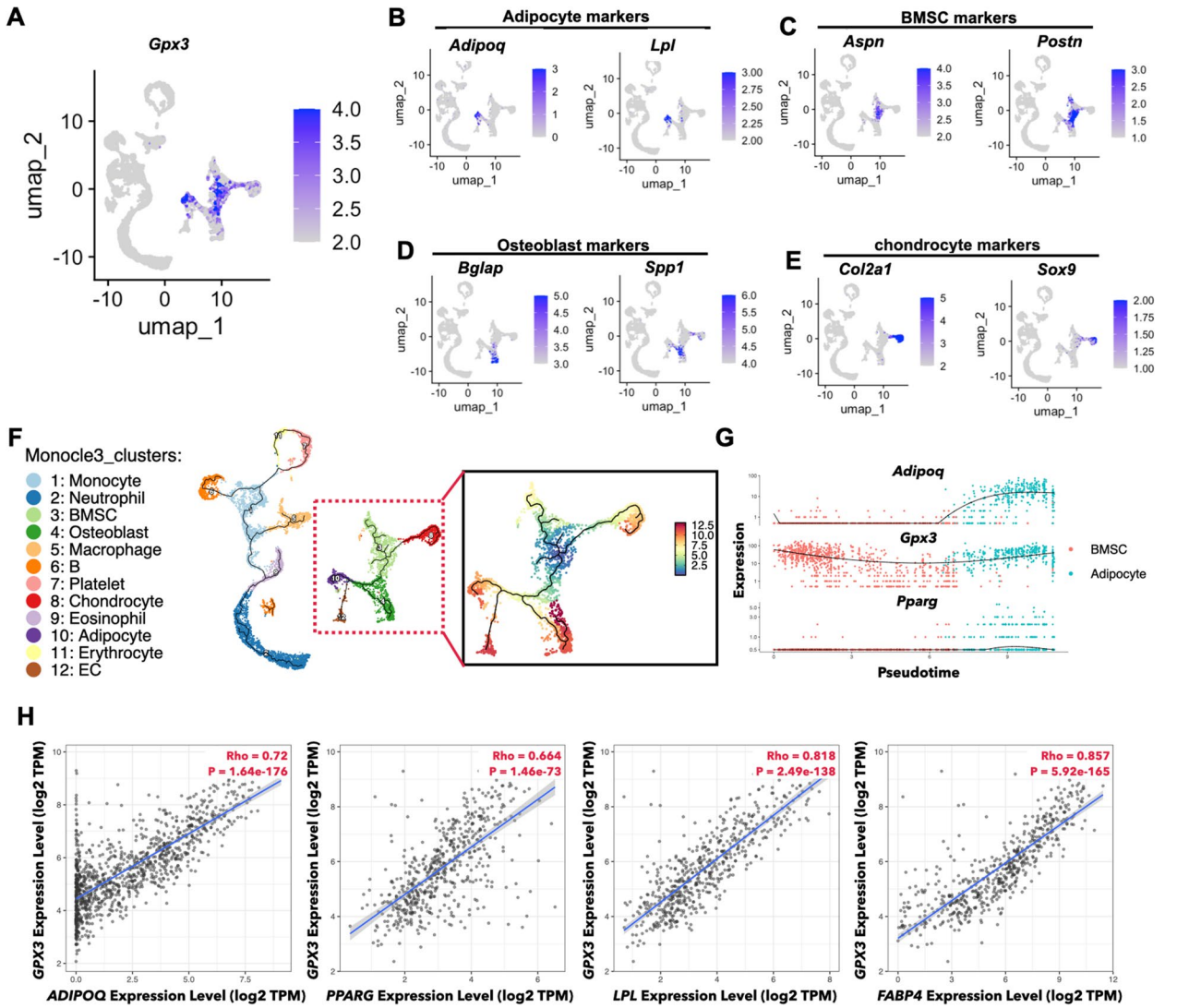

Fig. 4 Positive correlation between GPx3 expression and adipocytes. **A**-**E** scRNA-seq analysis of mouse bone marrow cells, visualized using UMAP dimensionality reduction, showing the expression levels of *Gpx3* in adipocytes (**B**), mesenchymal stem cells (**C**), osteoblasts (**D**) and chondrocytes (**E**). **F** UMAP visualization of cell clusters derived from Monocle3 analysis. **G** Pseudotime analysis of gene expression in BMSCs and adipocytes. **H** Correlation analysis between *GPX3* and adipogenesis marker genes in tumor cells based on the TIME2.0 database

Discussion

Previous studies on osteoporosis have primarily focused on the functions of osteoblasts and osteoclasts, while the roles of BMAT have often been overlooked. Although BMAT was historically considered an inert component of the bone marrow, accumulating evidence now positions it as a metabolically active tissue with dynamic roles in bone remodeling and marrow homeostasis [2, 20, 21]. Notably, BMAT expansion has been implicated in bone fragility, particularly in ageing and osteoporotic conditions, and genetic depletion of bone marrow adipocytes has led to remarkable gains in bone mass and strength [9]. These insights suggest that BMAT is not merely a bystander but a potentially modifiable contributor to bone loss—thereby opening new therapeutic avenues. However, the molecular mechanisms governing BMAT formation or adipogenic differentiation remain incompletely understood.

In this study, we revisited published transcriptomic data and revealed that the activation of oxidative stress-related pathways as being closely associated with the adipogenic differentiation of BMSCs. ROS contributes to oxidative stress have emerged as key modulators of adipogenic differentiation, functioning as signalling intermediates that activate pro-adipogenic transcription factors (e.g., C/EBPβ) [13]. Oxidative stress is highly related with increased lipid droplet formation [22], which is a key feature of adipocyte differentiation. In turn, lipid droplet could serve as a protective mechanism in response

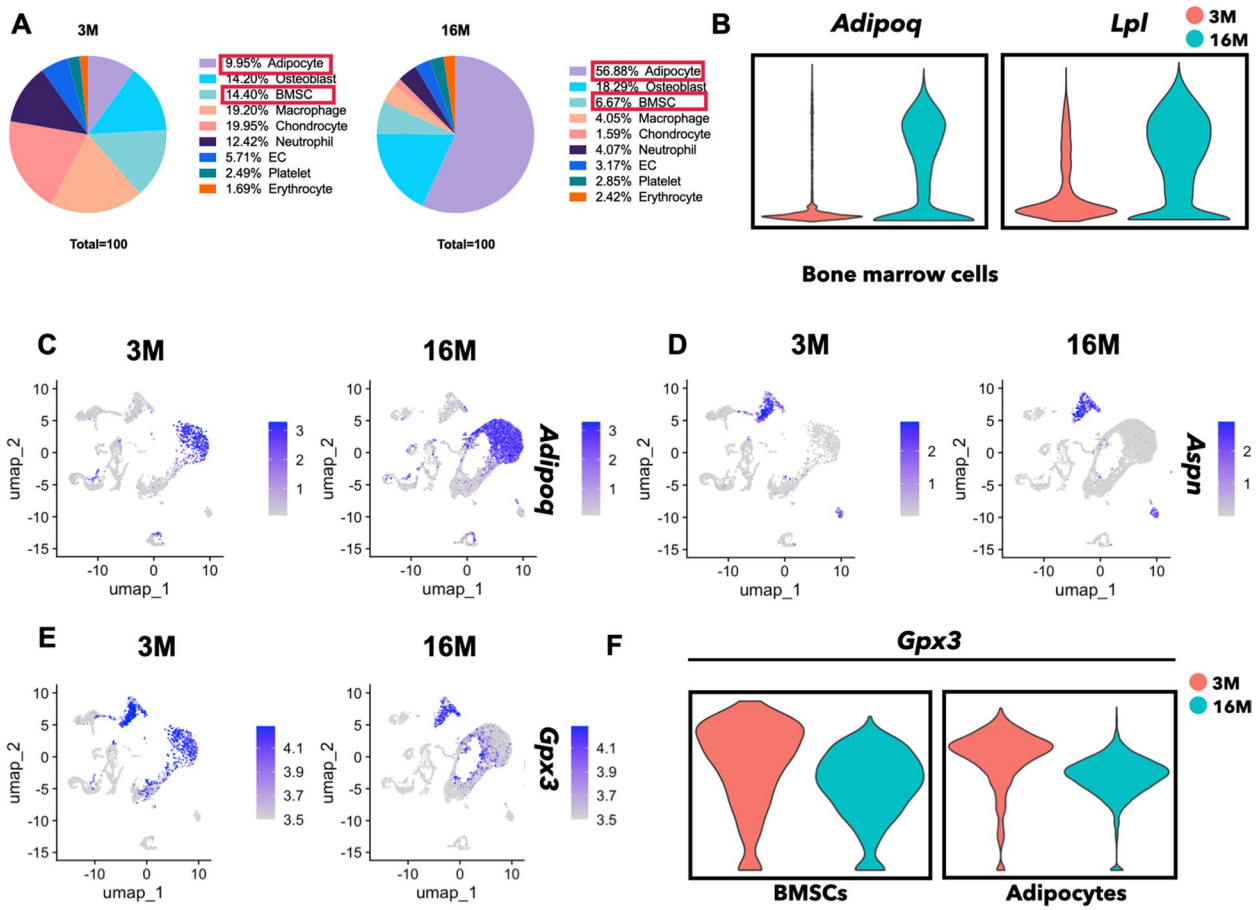

Fig. 5 scRNA-seq data indicates that increased BMAds is associated with diminished *Gpx3* expression during ageing. **A** The proportion of bone marrow cells in the young and aged bone marrow. **B** The expression levels of *Adipoq* or *Lpl* in the young and aged bone marrow. **C**-**E** UMAP visualization of *Adipoq* (adipocyte marker), *Aspn* (BMSC marker) and *Gpx3* expression in scRNA-seq data from bone marrow cells of mice at different ages. **F** The expression levels of *Gpx3* in BMSCs and adipocytes in the young and aged mice. 3 M, three-month-old mice; 16 M, sixteen-month-old mice; EC, endothelial cell

to excessive oxidative stress which can be cytotoxic [22, 23]. To maintain redox homeostasis, elevated oxidative stress is typically accompanied by the upregulation of antioxidant enzymes that help restore cellular and tissue redox balance [24]. We therefore investigated which antioxidant enzymes are specifically expressed during BMSC adipogenesis. Interestingly, among the GPx family members, GPx3 showed a distinct and robust increase in expression during adipogenic differentiation, as compared to osteogenic differentiation. GPx family comprises eight members (GPx1-8) and most GPx isoforms function intracellularly [24]. For example, GPx1 localizes to the cytosol and mitochondria, while GPx4 is membrane-associated and protects against lipid peroxidation. GPx3, however, is unique as the only member that is extracellularly secreted. Previous studies indicated that GPx3 is mainly expressed by renal tubular endothelial cells and circulates in plasma, where it functions as a major systemic antioxidative enzyme [16, 25]. More importantly, recent evidence indicated that GPx3 is critical for insulin receptor expression and sensitivity in peripheral adipose tissue [26]. Here, we found that GPx3 is highly expressed during BMSC adipogenesis, suggesting it may play a critical role in BMAds formation and serve as a potential biomarker for BMAT and bone homeostasis.

We next analysed scRNA-seq data from a published dataset in which Td^+ labelling was used for lineage tracing. Distinct cellular clusters remained clearly identifiable, indicating that Td^+ labelling did not substantially impact the transcriptional profiles or clustering outcomes. Given both BMSCs and BMAds in our study are Td^+ cells, we assumed that the use of Td^+ labelling aligns with our experimental design and does not compromise the validity of our conclusions. We examined GPx3 expression within the bone marrow environment and found that it is predominantly expressed in BMSCs and adipocytes, in contrast to other cell lineages such as osteoblasts and chondrocytes. These findings strongly suggest a cell-type-specific role for GPx3

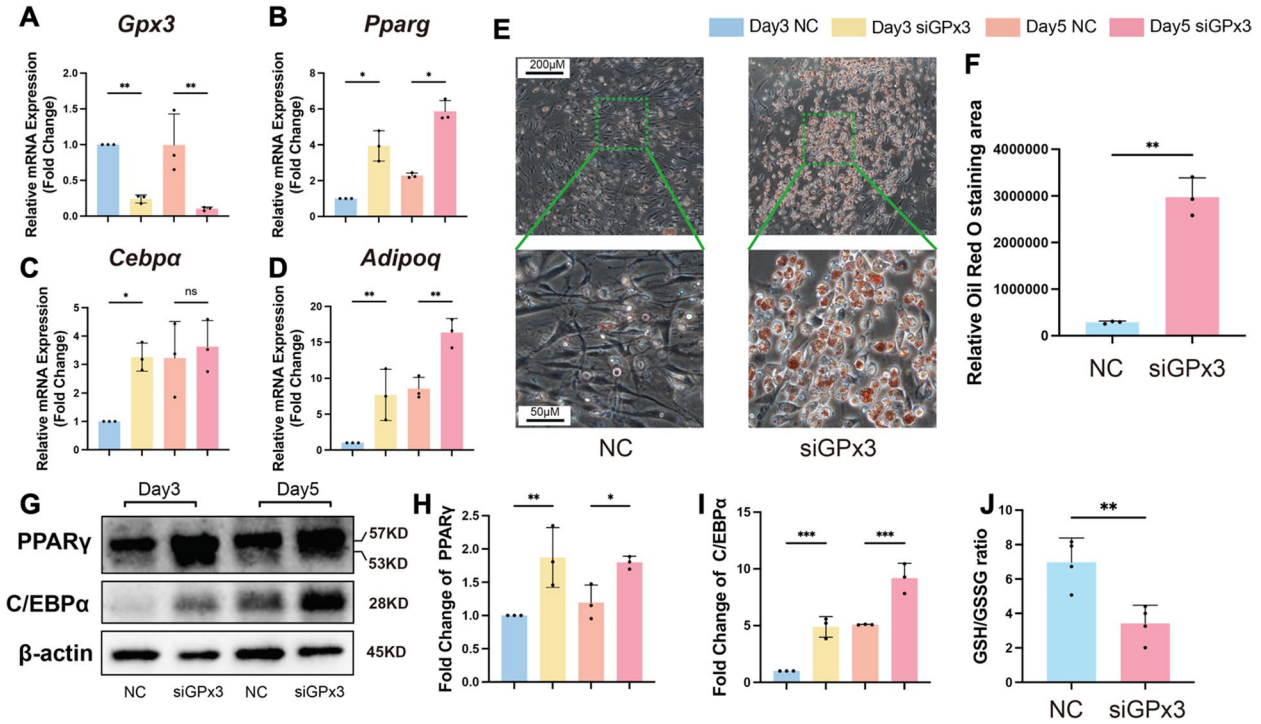

Fig. 6 Effect of GPx3 knockdown on adipogenic differentiation of mBMSCs. **A**-**D** Relative expression levels of *Gpx3, Pparg, Cebpa and Adipoq* genes normalized to *Actb* on days 3 and 5 of differentiation. **E** Representative images and (**F**) relative quantification of Oil Red O staining on day 5 of adipogenic differentiation. **G** Representative Western blot images and relative quantification of (**H**) PPARγ and (**I**) C/EBPα protein expression on days 3 and 5 of differentiation. **J** GSH/GSSG ratio on day 5 of adipogenic differentiation. Data are presented as mean ± SD. *$P < 0.05$, **$P < 0.01$, ***$P < 0.001$ compared to the control group; ns indicates $P > 0.05$

in the adipogenic differentiation of BMSCs. Moreover, analysis of the TIME2.0 database revealed a strong positive correlation between GPx3 and key adipocyte-related markers, including PPARG, LPL, and FABP4, further supporting its potential functional relevance in adipocyte formation. To investigate the relevance of GPx3 expression in BMAds to bone homeostasis, we re-analysed and compared single-cell transcriptomic profiles of bone marrow from young and aged mice. Our analysis revealed that aged bone marrow exhibits a reduced BMSC population and an increased adipocyte population, accompanied by global upregulation of adipocyte-related genes and a marked decrease in GPx3 expression within BMAds. These findings suggest that GPx3 may be essential for maintaining the BMSC phenotype, and that its downregulation could promote BMSC commitment to BMAds formation, contributing to ageing-associated bone loss.

Furthermore, using RNA interference, we knocked down GPx3 expression in BMSCs, as confirmed by qRT-PCR analysis, and observed that GPx3 deficiency significantly promoted adipogenic differentiation, potentially due to increased intracellular oxidative stress (Fig. 6). These results provide functional evidence that GPx3 acts as a negative regulator of adipogenic differentiation, highlighting its potential role in maintaining redox balance and controlling BMSC lineage commitment within the bone marrow niche.

The present study primarily focuses on establishing the association between GPx3 and BMSC commitment to adipogenic differentiation. We revealed that GPx3 may serve as a key ROS modulator of BMSC and is closely associated with adipocyte lineage commitment within the bone marrow microenvironment. However, there are several limitations, and further investigations are needed to elucidate the underlying mechanisms. First, although our findings demonstrate a functional role for GPx3 in regulating adipogenic differentiation in vitro, we have not yet confirmed its effects in vivo using genetic or preclinical models. Future studies employing conditional knockout or overexpression of GPx3 in BMSCs will be essential to establish its causal role in BMAT regulation and bone homeostasis. Second, while we observed a correlation between GPx3 expression and adipocyte markers in publicly available datasets, the underlying signaling pathways and molecular mechanisms through which GPx3 modulates redox status and lineage commitment remain to be elucidated. Additionally, our study focused primarily on mouse-derived cells, and further validation in human BMSCs or patient-derived bone marrow

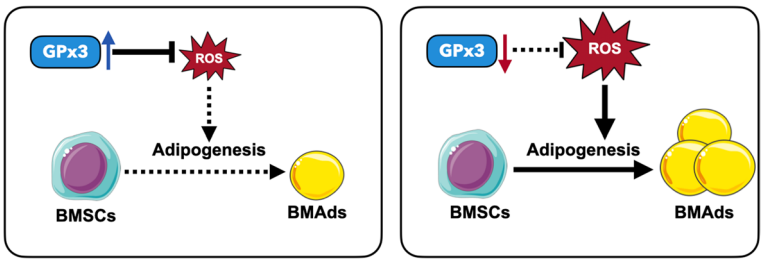

Fig. 7 A schematic diagram illustrating the proposed role of GPx3 in BMSC adipogenic differentiation and its underlying mechanism. During adipogenic differentiation, intracellular ROS levels increase and promote adipogenesis. GPX3 functions as a redox "checkpoint," attenuating ROS accumulation and thereby influencing BMSC lineage commitment

samples is needed to ensure translational relevance. Lastly, we measured ROS levels by assessing the GSH/GSSG ratio. However, downstream pathways activated by ROS remain unclear in this study and warrant future investigation.

Conclusions

In summary, through integrated transcriptomic analysis, in vitro validation, and functional knockdown experiments, we demonstrate that GPx3 is selectively upregulated during adipogenesis, and its suppression enhances adipogenic differentiation (Fig. 7). These findings suggest that GPx3 plays a critical role in maintaining redox balance and controlling BMSC lineage commitment, with potential implications for age-related bone marrow adiposity and osteoporosis. Targeting redox pathways such as GPx3 may offer new therapeutic strategies to limit BMAT accumulation and preserve skeletal health.

Supplementary Information

The online version contains supplementary material available at https://doi.org/10.1186/s13018-025-05908-8.

Supplementary Material 1. Figure S1. Quality control of bone marrow scRNA-seq data (GSE145477-1M). (A) The violin plots of feature_RNA, count_RNA and mitochondrial RNA. (B) FeatureScatter plot of mitochondrial RNA and count_RNA, as well as Feature_RNA and count_RNA. (C) The variable feature plot of all genes and the top 5 genes were marked. (D) Cells identified by scRNA-seq were visualized with UMAP. Different cell populations were defined and distinguished by color. (E) Violin plots of marker gene expression for different cell populations.

Supplementary Material 2. Figure S2. Quality control of bone marrow scRNA-seq data (GSE145477-3M VS 16M). (A) The violin plots of feature_RNA, count_RNA and mitochondrial RNA in 3M mice scRNA-seq data. (B) FeatureScatter plot of mitochondrial RNA and count_RNA, as well as Feature_RNA and count_RNA in 3M mice scRNA-seq data. (C) The variable feature plot of all genes in 3M mice scRNA-seq data and the top 5 genes were marked. (D) The violin plots of feature_RNA, count_RNA and mitochondrial RNA in 16M mice scRNA-seq data. (E) FeatureScatter plot of mitochondrial RNA and count_RNA, as well as Feature_RNA and count_RNA in 16M mice scRNA-seq data. (F) The variable feature plot of all genes in 16M mice scRNA-seq data and the top 5 genes were marked. (G) The UMAP of combined 3 and 16-month-old dataset and different cell populations were defined and distinguished by color. (H) Violin plots of marker gene expression for different cell populations.

Acknowledgements

The authors thank Professor Ling Qin and Professor Susanne Mandrup for sharing high-quality sequencing data, which served as a valuable foundation for the analyses and findings of this study. We also acknowledge the support of GraphPad Prism (version 10) and R (version 4.5.0) software in data analysis and visualization.

Authors' contributions

Conceptualization, K.C., L.W., and Z.W.; methodology, Z.W., K.C., Y.H., and X.C.; software, Z.W. C.Z. and X.C. validation, Z.W., Y.H., K.C., M.L., and L.W.; formal analysis, Z.W., X.C., M.L. and Z.X.; investigation, Z.W., Y.H., K.C., L.W. C.Z. and Z.X.; resources, K.C., L.W, and Z.W.; data curation, Y.H., Z.W. and K.C.; original draft preparation, Z.W., K.C., Y.H., and L.W.; review and editing, L.W., K.C., and Z.W.; visualization, Z.W., Y.H., X.C.; supervision, K.C. and L.W.; project administration, K.C. and L.W.; funding acquisition, K.C.. All authors have read and agreed to the published version of the manuscript.

Funding

This research was funded by Arthritis Australia, Raine Priming Grant (RPG001-2022), National Natural Science Foundation of China (82372368).

Data availability

The original contributions presented in the study are included in the article material, further inquiries can be directed to the corresponding author. The bioinformatics analysis data of hBMSCs undergoing osteogenic and adipogenic differentiation were obtained from the GEO database (GSE113253). Additionally, single-cell RNA sequencing data of mouse bone marrow were obtained from the GEO database (GSE145477).

Declarations

Ethics approval and consent to participate

The animal study protocol was approved by the Animal Ethics Committee of The University of Western Australia on 19 December 2022 (approval number 2022/ET000933).

Competing interests

The authors declare no competing interests.

Received: 15 April 2025 Accepted: 10 May 2025
Published online: 23 May 2025

References

1. Scheller EL, Cawthorn WP, Burr AA, Horowitz MC, MacDougald OA. Marrow Adipose Tissue: Trimming the Fat. Trends Endocrinol Metab. 2016;27(6):392–403. https://doi.org/10.1016/j.tem.2016.03.016.
2. Sebo ZL, Rendina-Ruedy E, Ables GP, Lindskog DM, Rodeheffer MS, Fazeli PK, Horowitz MC. Bone Marrow Adiposity: Basic and Clinical Implications. Endocr Rev. 2019;40(5):1187–206. https://doi.org/10.1210/er.2018-00138.

3. Suchacki KJ, Tavares AAS, Mattiucci D, Scheller EL, Papanastasiou G, Gray C, Sinton MC, Ramage LE, McDougald WA, Lovdel A, et al. Bone marrow adipose tissue is a unique adipose subtype with distinct roles in glucose homeostasis. Nat Commun. 2020;11(1):3097. https://doi.org/10.1038/s41467-020-16878-2.
4. Rosen CJ, Horowitz MC. Nutrient regulation of bone marrow adipose tissue: skeletal implications of weight loss. Nat Rev Endocrinol. 2023;19(11):626–38. https://doi.org/10.1038/s41574-023-00879-4.
5. Devlin MJ, Rosen CJ. The bone-fat interface: basic and clinical implications of marrow adiposity. Lancet Diabetes Endocrinol. 2015;3(2):141–7. https://doi.org/10.1016/S2213-8587(14)70007-5.
6. Veldhuis-Vlug AG, Rosen CJ. Clinical implications of bone marrow adiposity. J Intern Med. 2018;283(2):121–39. https://doi.org/10.1111/joim.12718.
7. Yu, W.; Zhong, L.; Yao, L.; Wei, Y.; Gui, T.; Li, Z.; Kim, H.; Holdreith, N.; Jiang, X.; Tong, W., et al. Bone marrow adipogenic lineage precursors promote osteoclastogenesis in bone remodeling and pathologic bone loss. J Clin Invest. 2021;131(2).https://doi.org/10.1172/JCI140214.
8. Inoue, K.; Qin, Y.; Xia, Y.; Han, J.; Yuan, R.; Sun, J.; Xu, R.; Jiang, J.X.; Greenblatt, M.B.; Zhao, B. Bone marrow Adipoq-lineage progenitors are a major cellular source of M-CSF that dominates bone marrow macrophage development, osteoclastogenesis, and bone mass. Elife. 2023;12. https://doi.org/10.7554/eLife.82118.
9. Zou, W.; Rohatgi, N.; Brestoff, J.R.; Li, Y.; Barve, R.A.; Tycksen, E.; Kim, Y.; Silva, M.J.; Teitelbaum, S.L. Ablation of Fat Cells in Adult Mice Induces Massive Bone Gain. Cell Metab. 2020;32(5):801–813 e806.https://doi.org/10.1016/j.cmet.2020.09.011.
10. Beekman KM, Duque G, Corsi A, Tencerova M, Bisschop PH, Paccou J. Osteoporosis and Bone Marrow Adipose Tissue. Curr Osteoporos Rep. 2023;21(1):45–55. https://doi.org/10.1007/s11914-022-00768-1.
11. Pittenger MF, Mackay AM, Beck SC, Jaiswal RK, Douglas R, Mosca JD, Moorman MA, Simonetti DW, Craig S, Marshak DR. Multilineage potential of adult human mesenchymal stem cells. Science. 1999;284(5411):143–7. https://doi.org/10.1126/science.284.5411.143.
12. Horowitz MC, Berry R, Holtrup B, Sebo Z, Nelson T, Fretz JA, Lindskog D, Kaplan JL, Ables G, Rodeheffer MS. et al. Bone marrow adipocytes. Adipocyte. 2017;6(3):193–204.https://doi.org/10.1080/21623945.2017.1367881.
13. Lee H, Lee YJ, Choi H, Ko EH, Kim JW. Reactive oxygen species facilitate adipocyte differentiation by accelerating mitotic clonal expansion. J Biol Chem. 2009;284(16):10601–9. https://doi.org/10.1074/jbc.M808742200.
14. Dzubanova M, Bond JM, Craige SM, Tencerova M. NOX4-reactive oxygen species axis: critical regulators of bone health and metabolism. Front Cell Dev Biol. 2024;12:1432668. https://doi.org/10.3389/fcell.2024.1432668.
15. Rauch A, Haakonsson AK, Madsen JGS, Larsen M, Forss I, Madsen MR, Van Hauwaert EL, Wiwie C, Jespersen NZ, Tencerova M, et al. Osteogenesis depends on commissioning of a network of stem cell transcription factors that act as repressors of adipogenesis. Nat Genet. 2019;51(4):716–27. https://doi.org/10.1038/s41588-019-0359-1.
16. Nirgude S, Choudhary B. Insights into the role of GPX3, a highly efficient plasma antioxidant, in cancer. Biochem Pharmacol. 2021;184:114365. https://doi.org/10.1016/j.bcp.2020.114365.
17. Love MI, Huber W, Anders S. Moderated estimation of fold change and dispersion for RNA-seq data with DESeq2. Genome Biol. 2014;15(12):550. https://doi.org/10.1186/s13059-014-0550-8.
18. Zhong, L.; Yao, L.; Tower, R.J.; Wei, Y.; Miao, Z.; Park, J.; Shrestha, R.; Wang, L.; Yu, W.; Holdreith, N., et al. Single cell transcriptomics identifies a unique adipose lineage cell population that regulates bone marrow environment. Elife. 2020;9. https://doi.org/10.7554/eLife.54695.
19. Lin W, Li Q, Zhang D, Zhang X, Qi X, Wang Q, Chen Y, Liu C, Li H, Zhang S, et al. Mapping the immune microenvironment for mandibular alveolar bone homeostasis at single-cell resolution. Bone Res. 2021;9(1):17. https://doi.org/10.1038/s41413-021-00141-5.
20. Liu, X.; Gu, Y.; Kumar, S.; Amin, S.; Guo, Q.; Wang, J.; Fang, C.L.; Cao, X.; Wan, M. Oxylipin-PPARgamma-initiated adipocyte senescence propagates secondary senescence in the bone marrow. Cell Metab. 2023;35(4):667–684 e666.https://doi.org/10.1016/j.cmet.2023.03.005.
21. Li Z, Hardij J, Bagchi DP, Scheller EL, MacDougald OA. Development, regulation, metabolism and function of bone marrow adipose tissues. Bone. 2018;110:134–40. https://doi.org/10.1016/j.bone.2018.01.008.
22. Zadoorian A, Du X, Yang H. Lipid droplet biogenesis and functions in health and disease. Nat Rev Endocrinol. 2023;19(8):443–59. https://doi.org/10.1038/s41574-023-00845-0.
23. Olzmann JA, Carvalho P. Dynamics and functions of lipid droplets. Nat Rev Mol Cell Biol. 2019;20(3):137–55. https://doi.org/10.1038/s41580-018-0085-z.
24. Pei J, Pan X, Wei G, Hua Y. Research progress of glutathione peroxidase family (GPX) in redoxidation. Front Pharmacol. 2023;14:1147414. https://doi.org/10.3389/fphar.2023.1147414.
25. Zhao L, Zong W, Zhang H, Liu R. Kidney Toxicity and Response of Selenium Containing Protein-glutathione Peroxidase (Gpx3) to CdTe QDs on Different Levels. Toxicol Sci. 2019;168(1):201–8. https://doi.org/10.1093/toxsci/kfy297.
26. Hauffe, R.; Stein, V.; Chudoba, C.; Flore, T.; Rath, M.; Ritter, K.; Schell, M.; Wardelmann, K.; Deubel, S.; Kopp, J.F., et al. GPx3 dysregulation impacts adipose tissue insulin receptor expression and sensitivity. JCI Insight. 2020;5(11).https://doi.org/10.1172/jci.insight.136283.

Publisher's Note